# Robust superconducting state in the low-quasiparticle-density organic metals $\beta''$-(BEDT-TTF)$_4$[$(H_3O)M(C_2O_4)_3$]$\cdot Y$: Superconductivity due to proximity to a charge-ordered state

A. F. Bangura and A. I. Coldea
*Clarendon Laboratory, University of Oxford, Parks Road, Oxford OX1 3PU, United Kingdom*

J. Singleton
*National High Magnetic Field Laboratory, Los Alamos National Laboratory, TA-35, MS-E536, Los Alamos, New Mexico 87545, USA*

A. Ardavan
*Clarendon Laboratory, University of Oxford, Parks Road, Oxford OX1 3PU, United Kingdom*

A. Akutsu-Sato,* H. Akutsu,† S. S. Turner, and P. Day
*Davy-Faraday Research Laboratory, The Royal Institution, 21 Albemarle Street, London, W1X 4BS, United Kingdom*

T. Yamamoto and K. Yakushi
*Institute for Molecular Science, Myodaiji, 444-8585 Okazaki, Japan*
(Received 7 September 2004; revised manuscript received 9 June 2005; published 27 July 2005)

We report magnetotransport measurements on the quasi-two-dimensional charge-transfer salts $\beta''$-(BEDT-TTF)$_4$[$(H_3O)M(C_2O_4)_3$]$Y$, with $Y=C_6H_5NO_2$ and $C_6H_5CN$ using magnetic fields of up to 45 T and temperatures down to 0.5 K. A surprisingly robust superconducting state with an in-plane upper critical field $B_{c2\|}\approx 33$ T, comparable to the highest critical field of any BEDT-TTF superconductor, and critical temperature $T_c\approx 7$ K is observed when $M=$Ga and $Y=C_6H_5NO_2$. The presence of magnetic $M$ ions reduces the in-plane upper critical field to $\approx 18$ T for $M=$Cr and $Y=C_6H_5NO_2$ and $M=$Fe and $Y=C_6H_5CN$. Prominent Shubnikov–de Haas oscillations are observed at low temperatures and high magnetic fields, showing that the superconducting salts possess Fermi surfaces with one or two small quasi-two-dimensional pockets, their total area comprising $\lesssim 6\%$ of the room-temperature Brillouin zone; the quasiparticle effective masses were found to be enhanced when the ion $M$ was magnetic (Fe or Cr). The low effective masses and quasiparticle densities, and the systematic variation of the properties of the $\beta''$-(BEDT-TTF)$_4$[$(H_3O)M(C_2O_4)_3$]$Y$ salts with unit-cell volume points to the possibility of a superconducting groundstate with a charge-fluctuation-mediated superconductivity mechanism such as that proposed by Merino and McKenzie [Phys. Rev. Lett. **87**, 237002 (2001)], rather than the spin-fluctuation mechanism appropriate for the $\kappa$-(BEDT-TTF)$_2X$ salts.

DOI: 10.1103/PhysRevB.72.014543 PACS number(s): 74.10.+v, 71.18.+y, 71.20.Rv, 72.15.Gd

## I. INTRODUCTION

There have been a number of recent suggestions that there may be two[1,2] or possibly three[3] distinct mechanisms for superconductivity in quasi-two-dimensional crystalline organic metals. The $\kappa$-(BEDT-TTF)$_2X$ family of salts has been most heavily studied; their low-temperature superconducting phase emerges with increasing pressure from an antiferromagnetic state[4] that exhibits behavior[5] characteristic of a Mott insulator.[6] Subsequent increases of pressure gradually suppress the superconductivity, the suppression being linked to a fall in the quasiparticle density-of-states close to the Fermi energy[7,8] and an increase in the effective dimensionality of the Fermi surface.[9,10] A greater proportion of the experimental data and theoretical models suggest that the superconductivity in $\kappa$-(BEDT-TTF)$_2X$ is non-BCS-like, perhaps mediated by spin fluctuations (for a summary, see Refs. 2, 3, and 11, and citations therein), although this view is by no means universal (see, e.g., Refs. 12 and 13).

A second mechanism for superconductivity, applicable to (BEDT-TTF) charge-transfer salts with the $\beta''$ or $\theta$ structures, has been suggested by Merino and McKenzie.[1] Slave-boson theory was applied to an extended Hubbard model for a system in which competition between charge-ordered and metallic phases can occur;[1] the resulting superconductivity is mediated by *charge* fluctuations, rather than the spin fluctuations thought to occur in the $\kappa$-(BEDT-TTF)$_2X$ salts.[2] However, in contrast to the case of the latter superconductors, BEDT-TTF salts with the $\beta''$ structure have been examined in only a small number of cases.

In this paper, we report a study of the superconductivity and Fermi-surface topology of a series of salts with the $\beta''$ structure, of general formula $\beta''$-(BEDT-TTF)$_4$[$(H_3O)M(C_2O_4)_3$]$\cdot Y$. In this family, the properties can be tuned by changing the metal ion $M$ ($M=$Ga, Cr or Fe are possible) and/or the guest molecule $Y$, which resides in the anion layer; $Y$ can be $C_5H_5N$ (pyridine), $C_6H_5CN$ (benzonitrile), or $C_6H_5NO_2$ (nitrobenzene). In spite of an exceptionally small quasiparticle density of states, some of these salts exhibit a very robust superconducting state with maximum upper critical fields around 33 T. This observation is in direct contrast to the $\kappa$-(BEDT-TTF)$_2X$ salts, where the supercon-

 

ductivity is associated with a large quasiparticle density of states,[2,3] and suggests that superconductivity in the $\beta''$-(BEDT-TTF)$_4$[$(H_3O)M(C_2O_4)_3$]$\cdot Y$ family may well be driven by a different mechanism, which we tenetatively suggest may be that described in Ref. 1. Support for this assertion is given by the dependence of the properties of the salts on crystallographic unit cell size, varied by altering $Y$ and $M$, and the evidence of charge ordering in the BEDT-TTF layer observed in Raman data. This paper concentrates on the superconducting salts which have $Y=C_6H_5CN$ and $C_6H_5NO_2$ (the related nonsuperconducting salts with $Y=C_5H_5N$ are described in a companion paper[14]) and is organized as follows. Section II covers the experimental arrangements for measuring the resistivity of the $\beta''$-(BEDT-TTF)$_4$[$(H_3O)M(C_2O_4)_3$]$\cdot Y$ crystals in steady magnetic fields of up to 45 T and at temperatures as low as 500 mK, and describes the experimental setup used to acquire the Raman data. The results are described in Sec. III, which comprises several subsections. Sections III A and III B discuss how the transport properties of these compounds can be understood by proposing that they are electronically inhomogeneous, consisting of coexisting metallic and insulating phases (see also Ref. 14). In spite of this "intrinsic disorder,"[14] the observation of Shubnikov–de Haas oscillations (Secs. III C and III D) shows that all of the superconducting salts possess Fermi surfaces with one or two small quasi-two-dimensional pockets, their total area comprising $\lesssim 6\%$ of the room-temperature Brillouin zone. The quasiparticle effective masses were found to be enhanced when the ion $M$ was magnetic (Fe or Cr); this is in contrast to the behavior of the related nonsuperconducting salts,[14] in which there was no systematic dependence of the effective mass on $M$. In spite of the very low quasiparticle density [$\lesssim 10\%$ of that in the $\kappa$-(BEDT-TTF)$_2X$ salts] and their relatively small effective masses $\sim\frac{1}{6}-\frac{1}{4}$ of those in the $\kappa$ phase salts), superconductivity is observed below $T_c \approx 7$ K, with in-plane upper critical fields of up to 33 T (Secs. III E and III F), comparable to the highest critical fields of *any* BEDT-TTF superconductor.[15] The magnetic ions Fe and Cr were found to reduce the in-plane upper critical field compared to that observed when $M=$Ga, possibly due to exchange interactions between the localized ions and the itinerant charge carriers. Finally, Sec. IV compares the magnetotransport results on the $\beta''$-(BEDT-TTF)$_4$[$(H_3O)M(C_2O_4)_3$]$\cdot Y$ salts, in the light of the charge ordering evidence observed in the temperature-dependent Raman data presented in this section, with the notional phase diagram for charge-fluctuation-mediated superconductivity proposed in Ref. 1. A summary is given in Sec. V.

## II. EXPERIMENTAL DETAILS

The $\beta''$-(BEDT-TTF)$_4$[$(H_3O)M(C_2O_4)_3$]$\cdot Y$ samples were grown using electrocrystallisation techniques as described elsewhere;[14,16–18] they are generally $\sim 3\times 1\times 0.5$ mm$^3$ needles. It is possible to deduce the upper and lower faces that are parallel to the highly conducting quasi-two-dimensional planes by visual inspection. Electrical contacts were made to these surfaces by using graphite paint to attach 12-$\mu$m platinum wires. The interlayer (magneto)resistance $R_{zz}\propto\rho_{zz}$ (Ref. 3) was measured using standard four-terminal ac techniques. This involves driving the current and measuring the voltage between pairs of contacts on the upper and lower surfaces.[3] Magnetoresistance experiments were carried out in quasistatic fields provided by a superconductive magnet in Oxford and a 33 T Bitter coil and the 45 T Hybrid magnet at NHMFL Tallahassee. The crystals were mounted in a $^3$He cryostat which allowed rotation to all possible orientations in magnetic field; sample orientation is defined by the angle $\theta$ between the direction of the magnetic field and the normal ($c^*$) to the quasi-two-dimensional ($ab$) planes. Sample currents between 1 and 25 $\mu$A were used at typical frequencies 18–300 Hz. Although around 15 crystals have been studied, in this paper we shall focus on two or three typical samples of each salt.

Raman spectra were measured on a Renishaw Ramascope system-1000 with a backward-scattering configuration. The conducting planes of a $\beta''$-(BEDT-TTF)$_4$[$(H_3O)Ga(C_2O_4)_3$]$\cdot C_6H_5NO_2$ single crystal were excited by diode laser (780 nm), and the resolution of the spectrometer was 2 cm$^{-1}$. The sample was cooled using a continuous-flow helium cryostat manufactured by Oxford Instruments (CF1104s). Detailed experimental procedures for the Raman study are described elsewhere.[19] A general description of the layered structure of the $\beta''$-(BEDT-TTF)$_4$[$(H_3O)M(C_2O_4)_3$]$\cdot Y$ compounds together with crystallographic details and lattice parameters is given in the companion paper covering the nonsuperconducting salts.[14]

## III. EXPERIMENTAL RESULTS

### A. Temperature dependence of the zero-field resistivity

Figure 1 shows the interlayer resistivity $\rho_{zz}(T)$ of a selection of $\beta''$-(BEDT-TTF)$_4$[$(H_3O)M(C_2O_4)_3$]$\cdot Y$ samples as a function of temperature $T$. For ease of comparison, all data have been normalized to the room-temperature value $\rho_{zz}(T=293$ K). We first discuss the salts which exhibit superconductivity, shown in Figs. 1(a)–1(c) and later return to the $M=$Fe, $Y=C_6H_5NO_2$ sample shown as an inset to Fig. 1.

In spite of some very obvious variations from sample to sample (and amongst samples of the same chemical composition),[20] there are a number of features common to all of the materials featured in Figs. 1(a)–1(c) ($Y=C_6H_5NO_2$, $M=$Cr, Ga; $Y=C_6H_5CN$, $M=$Fe). On cooling from room temperature, $\rho_{zz}(T)$ at first falls in a fashion characteristic of a metal ($d\rho_{zz}/dT>0$) before reaching a minimum at a temperature that we label $T_{MI}$. Below $T_{MI}$, $\rho_{zz}(T)$ shows behavior characteristic of an insulator ($d\rho_{zz}/dT<0$); however, eventually, at $T\sim 10$ K, the resistivity peaks in all samples, and there is an indication of the onset of superconductivity. Defining the critical temperature $T_c$ as the point at which $\rho_{zz}$ peaks (this choice will be discussed in Sec. III B) yields the values shown in the first row of Table I; the uncertainty shown represents the spread of values between the various measurements and/or the difficulty of precisely locating the peak, rather than an error in the temperature.

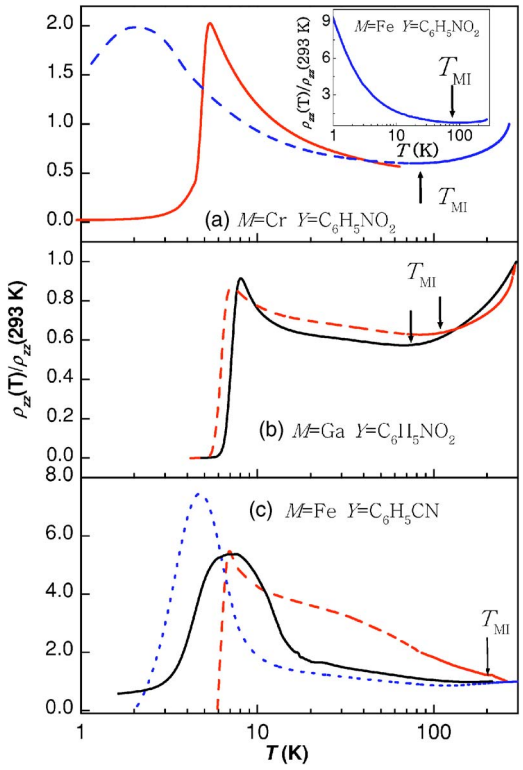


FIG. 1. (Color online) The temperature ($T$) dependence of the interplane component of the resistivity $\rho_{zz}(T)$ for several typical $\beta''$-(BEDT-TTF)$_4$[$(H_3O)M(C_2O_4)_3$]·$Y$ samples at zero magnetic field; data for different samples of the same material are shown by distinct types of curve (dashed, solid). Data are shown for (a) $M$=Cr and $Y$=$C_6H_5NO_2$, (b) $M$=Ga and $Y$=$C_6H_5NO_2$, and (c) $M$=Fe and $Y$=$C_6H_5CN$. The inset shows the resistivity of a typical $\beta''$-(BEDT-TTF)$_4$[$(H_3O)Fe(C_2O_4)_3$]·$C_6H_5NO_2$ sample. For ease of comparison, all $\rho_{zz}$ are normalized to the room-temperature value $\rho_{zz}$(293 K). The arrow indicates the temperature $T_{MI}$ at which $d\rho_{zz}/dT$ changes from negative (characteristic of insulating properties) to positive (characteristic of metallic behavior).

Most of the samples show $\rho_{zz}\rightarrow 0$ for sufficiently low temperatures, but there are examples [e.g., Figs. 1(a) and 1(c)] in which $\rho_{zz}$ is finite even as $T\rightarrow 0$. Similar phenomena have been observed in organic superconductors in which insulating and superconducting states compete[21] and in other disordered superconductors (e.g., Ref. 22).

Turning to the minimum in resistivity at $T_{MI}$, exhibited by all of the samples, we remark that this may, by analogy with the $\beta''$-(BEDT-TTF)$_4$[$(H_3O)M(C_2O_4)_3$]·$Y$ salts with $Y$=$C_6H_5N$,[14] represent the onset of some form of density-wave state. Quasi-two-dimensional conductors in which the Fermi surface is completely gapped by a density wave exhibit a resistivity that rises by several orders of magnitude as the temperature falls [an example is (BEDT-TTF)$_3Cl_2$.2$H_2O$ (Ref. 21)]; by contrast, the resistances of the salts featured in Figs. 1(a)–1(c) only increase by a factor $\sim$1.5–8. The latter behavior is similar to that of quasi-two-dimensional conductors in which a density wave only partially nests the Fermi surface, leaving behind residual Fermi-surface pockets; examples include the Mo bronzes[23] and $\alpha$-(BEDT-TTF)$_2$KHg(SCN)$_4$.[24] In such cases, the conductivity is a convolution of a metallic component, typically varying as a power law in temperature (due to the unnested portions of the Fermi surface) and an insulating component with an activated temperature dependence (due to the energy gap of the density-wave state);[9] the exact form of the resistivity will depend on which component dominates.

A more likely scenario that could potentially lead to much the same resistivity behavior is the segregation of the sample into insulating and metallic-superconducting domains,[14,25] with the insulating regions (again, perhaps due to density-wave formation) forming at the characteristic temperature $T_{MI}$. This mixture of phases may be the consequence of the mechanisms for intrinsic disorder, both static and dynamic, known to occur in the $\beta''$-(BEDT-TTF)$_4$[$(H_3O)M(C_2O_4)_3$]·$Y$ salts.[14] In the case of the $Y$=$C_6H_5CN$ and $C_6H_5NO_2$ compounds, the chief culprit is the variety of staggered, eclipsed or twisted configurations that the terminal ethylene groups of the BEDT-TTF molecules can adopt with little or no energy penalty.[14] Local variations in crystal structure could lead to regions that are either predisposed to remain metallic or form an insulating state such as a density wave.[14,25] Additional support for this picture of coexisting "insulating" and "metallic" regions is given by the rather varied behavior of samples with nominally the same composition [see, e.g., Figs. 1(a)–1(c)], which could be explained by variations in the relative proportions of the two components.

The relative change in $\rho_{zz}$ between room temperature and the peak close to $T_c$ varies significantly from $\sim$1 for $M$=Ga, $Y$=$C_6H_5NO_2$ [Fig. 1(b)] through $\sim$2 for $M$=Cr, $Y$=$C_6H_5NO_2$ [Fig. 1(a)] to $\sim$8 for $M$=Fe, $Y$=$C_6H_5CN$ [Fig. 1(c)]. This suggests that the fraction of the metallic component decreases and the activated, insulating regions start to dominate as the composition changes from $M$=Ga to Fe. To acquire a more quantitative description of this effect, we have fitted the conductivity over a limited temperature range just below $T_{MI}$ to a simple parallel-conduction expression

$$\sigma = \frac{A}{T^{\eta}} + C\exp\left(-\frac{E_A}{k_B T}\right). \quad (1)$$

Here, the first term on the right-hand side describes the metallic conduction (the parameter $\eta\sim 1-3$) and the second term represents the insulating component, with characteristic activation energy $E_A$. The constants $A$ and $C$ parametrize the relative sizes of the two components. The fitted $E_A$ is smallest for $M$=Ga, $Y$=$C_6H_5NO_2$, and largest for $M$=Fe, $Y$=$C_6H_5CN$; a qualitatively similar variation in $T_{MI}$ is also observed, with $T_{MI}\approx 70\pm 10$ K for $M$=Ga, Cr, $Y$=$C_6H_5NO_2$ to higher temperatures for $M$=Fe, $Y$=$C_6H_5CN$ ($T_{MI}\sim 120$ K).

Finally, we turn to the inset to Fig. 1, which shows data for $M$=Fe, $Y$=$C_6H_5NO_2$. In this study, six different samples with this composition were measured with all but one found to exhibit a strong insulatinglike behavior across the full temperature range, i.e., negative $d\rho_{zz}/dT$. However, in concurrence with the study reported in Ref. 26, one of the samples measured was superconducting, with $T_c\approx 7$ K. The activation energies of this salt were found to be the largest of

TABLE I. Parameters of three salts with generic chemical formula $\beta''$-(BEDT-TTF)$_4$[$(H_3O)M(C_2O_4)_3$]$\cdot Y$. Three examples of each salt with different $M$ are presented: $Y$ is identical for two of the salts. $T_c$ is the critical temperature for the onset of superconductivity, $T_{MI}$ is the characteristic "metal-insulting" transition temperature shown in Fig. 1and $E_A$ is the activation energy discussed in Sec. III A. $F_{\alpha,\delta}$,$m^*_{\alpha,\delta}$, and $T_{D(\delta)}$ are frequencies of the Shubnikov–de Haas oscillations, quasiparticle effective masses, and Dingle temperatures, respectively, associated with the $\alpha$ and $\delta$ Fermi surface pockets discussed in Sec. III C. $g^*m^*$ is the product of the effective $g$-factor and the effective mass; with $B_{c2\parallel}$(T) and $B_{c2\perp}$(T), the upper critical field with the magnetic field $B$ directed perpendicular or parallel to the $ab$ plane, respectively.

| $M$ | Cr (A) | Cr(B) | Cr(C) | Ga(A) | Ga(B) | Ga(C) | Fe(A) | Fe(B) | Fe(C) |
|---|---|---|---|---|---|---|---|---|---|
| $Y$ | $C_6H_5NO_2$ | $C_6H_5NO_2$ | $C_6H_5NO_2$ | $C_6H_5NO_2$ | $C_6H_5NO_2$ | $C_6H_5NO_2$ | $C_6H_5CN$ | $C_6H_5CN$ | $C_6H_5CN$ |
| $T_c$(K) | 6±0.5 | 3.5±1 | 5.3±1 | 7±0.5 | 8±1 | 8±1 | 6.5±0.5 | 4.7±0.5 | 6±1 |
| $T_{MI}$(K) | 89 | 94 | 88 | 68 | 69 | | 154 | 124 | |
| $E_A/k_B$(K) | 14±3 | | | 6±0.5 | | | 22±3 | | |
| $F_\alpha$(T) | | | | | | | 58 | 55 | 57±5 |
| $F_\delta$(T) | 223±20 | 223±25 | 227±25 | 220±10 | 230±10 | 210±10 | 192 | 192 | 192±10 |
| $m^*(m_e)_{(\alpha)}$ | | | | | | | 1.4±0.1 | 1.4±0.1 | |
| $m^*(m_e)_{(\delta)}$ | 1.9±0.1 | 1.7±0.1 | 1.7±0.1 | 1.3±0.1 | 1.2±0.2 | | 1.6±0.2 | 1.6±0.1 | |
| $T_{D(\delta)}$(K) | 1.8±0.3 | 4±0.5 | 3.5±0.5 | 3.8±0.1 | 5.1±0.2 | 5.5±0.5 | 2.6±0.5 | 2.8±0.5 | 2.8±0.4 |
| $g^*m^*$ | | | | 2.12±0.05 | | | | 1.8±0.1 | |
| $B_{c2\parallel}$(T) | 11.8 (at 2 K) | | 18.2 | 33.4±0.2 | 32 | 31 | 17.5±0.2 | 18.6 | 16±1 |
| $B_{c2\perp}$(T) | 1.7 (at 2 K) | | 2.2 | 5.2±0.05 | 6.5 | 5.9 | 3.3±0.1 | 3.6 | |

all the salts studied, with $E_A/k_B \approx 30$ K (cf. Table I).

In summary, the temperature dependence of the resistance of the $\beta''$-(BEDT-TTF)$_4$[$(H_3O)M(C_2O_4)_3$]$\cdot Y$ salts shown in Fig. 1 is characteristic of the coexistence of metallic-superconducting and insulating behavior, the latter being characterisable by a "metal-insulator" transition temperature $T_{MI}$ and an activation energy $E_A$. The resulting properties range from the most metallic tendencies (smallest $T_{MI}$ and $E_A$ of the $M$=Ga, $Y$=$C_6H_5NO_2$ salt), to those of the "insulating" $M$=Fe, $Y$=$C_6H_5NO_2$ compound. However, mechanisms for instrinsic disorder[14] also play a role, with substantial variations in the form of the resistivity being observed amongst samples of the same composition.

### B. Resistivity at finite magnetic field

Figure 2 shows the magnetic field ($B$) dependence of $\rho_{zz}$ at temperatures $T$ covering the range 1.4 to 50 K for a sample of $\beta''$-(BEDT-TTF)$_4$[$(H_3O)M(C_2O_4)_3$]$\cdot Y$ with $M$=Ga, $Y$=$C_6H_5NO_2$. Qualitatively similar behavior was observed for $M$=Cr, $Y$=$C_6H_5NO_2$ and $M$=Fe, $Y$=$C_6H_5CN$ samples. For $T \geqslant 10$ K, $\rho_{zz}$ is initially ($B \lesssim 3$ T) proportional to $B^2$; at higher fields, the resistivity varies approximately linearly with $B$. Such behavior is entirely typical of metallic charge-transfer salts[21,27] and other layered systems;[28,29] the magnetoresistance is presumably mainly associated with the metallic regions of the samples.

As the system approaches temperatures at which superconductivity is observed, a strong negative magnetoresistance develops at low fields. Negative magnetoresistance and an associated peak (in the interlayer resistivity) have been observed both as function of magnetic field and temperature in many organic and copper oxide superconductors below the superconducting transition temperature.[30–32] These features have been attributed to a number of mechanisms, including parallel conduction channels of stacked Josephson junctions between two-dimensional superconducting layers (i.e., a conduction channel arising from Cooper pair tunneling) and thermally activated quasiparticle tunneling between layers.[30,33] Although such models predict behavior in qualitative agreement with the data shown in Fig. 2, a satisfactory quantitative fit is not possible; in view of the inhomogeneous or mixed-phase nature of these salts, as discussed in Sec. III A, this is perhaps hardly surprising. Moreover, with $M$=Cr and $Y$=$C_6H_5NO_2$, when the field is directed perpendicular to the $ab$ plane, the minimum of the negative magnetoresistance occurs at fields $\geqslant$33 T. This is at a far higher field than any of the other features in the magnetoresistance that can be associated with superconductivity; for example, the characteristic downturn in $\rho_{zz}$ in an in-plane field [see Fig. 8(a)] suggestive of superconductivity[32] is completely absent at such values of $B$. This suggests that at least part of the observed negative magnetoresistance in these salts is due to another mechanism than superconductivity.

Irrespective of the exact mechanism, it is clear from previous measurements of organic superconductors (e.g., Ref. 36) that the peak in $\rho_{zz}$ is associated with the superconducting state; therefore, even though the resistivity does not reach zero, one can state that vestiges of the superconductivity remain in the sample of Fig. 2 up to $T \approx 8$ K. Faced with such a broad transition as a function of both field and temperature (zero resistance is observed at 2.5 K in Fig. 2, while the peak starts to develop at 8 K), we follow the precedent set by others[3] and associate $T_c$ in temperature sweeps and the upper critical field $B_{c2}$ seen in field sweeps with the peak in $\rho_{zz}$.

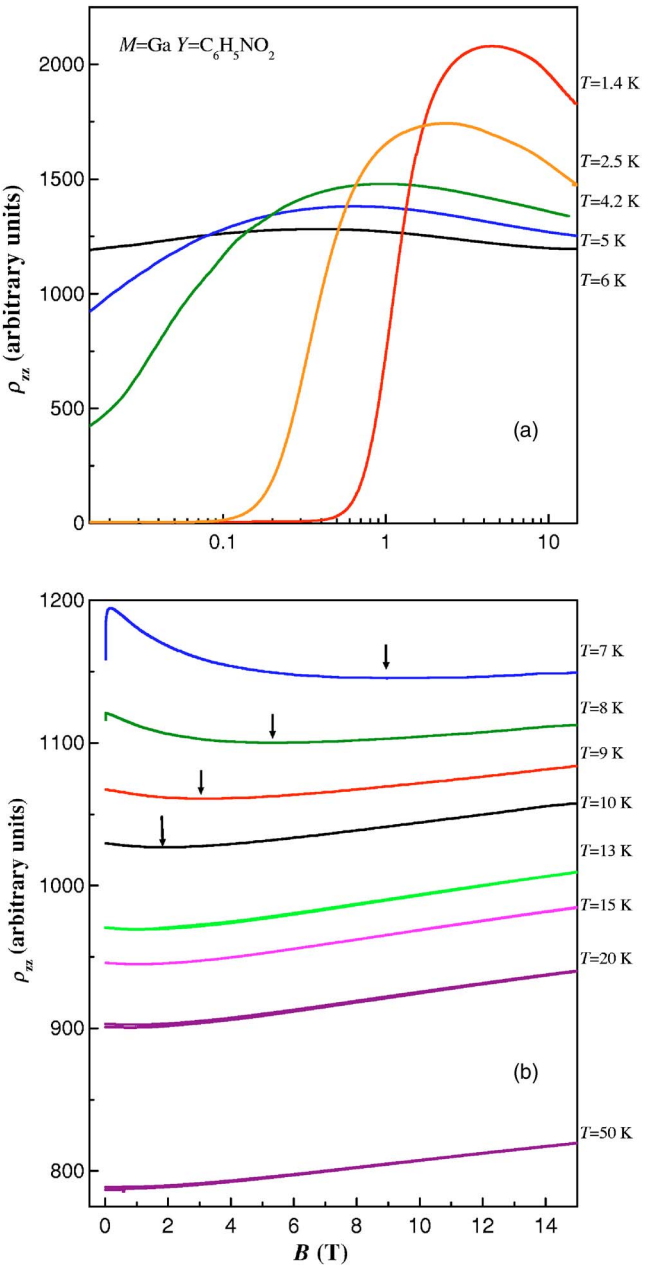


FIG. 2. (Color online) Field dependence of the interplane resistance ($B \| I \| c^*$) for $\beta''$-(BEDT-TTF)$_4$[$(H_3O)Ga(C_2O_4)_3$]·$C_6H_5NO_2$ at several fixed temperatures.

### C. Magnetic quantum oscillations

The interplane resistance, $\rho_{zz}$ at temperatures $T \leqslant 4.2$ K is shown as a function of magnetic field in Fig. 3 when the field was applied parallel to the $c^*$ direction, perpendicular to the conducting $ab$ planes ($\theta = 0°$). The use of higher fields than those applied in Fig. 2 allows Shubnikov–de Haas oscillations to be observed, superimposed on a slowly varying, slightly negative magnetoresistance.

The samples with $M$=Ga, $Y$=$C_6H_5NO_2$ [Fig. 3(b)] and $M$=Fe, $Y$=$C_6H_5CN$ [Fig. 3(c)] exhibit two distinct series of Shubnikov–de Haas oscillations, although the lower frequency oscillations are less well defined in the case of the

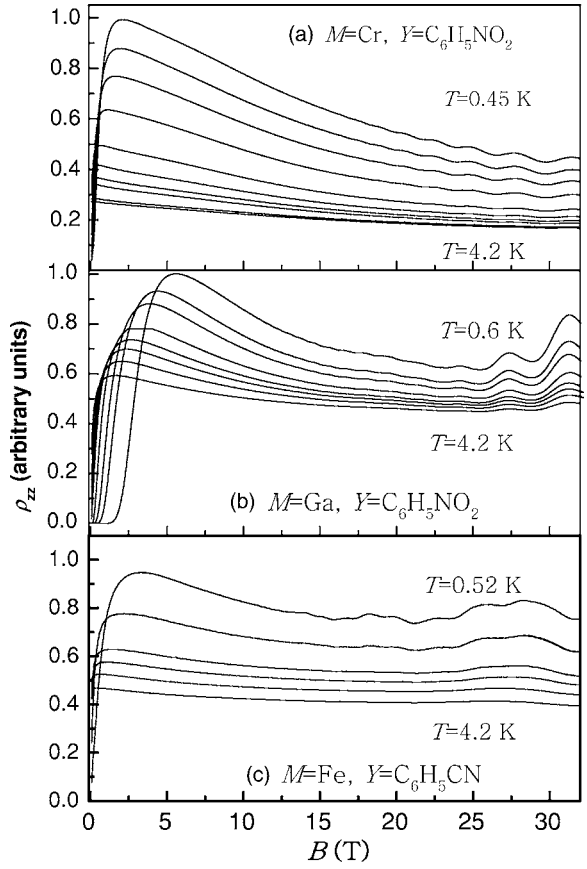


FIG. 3. The field dependence of the interplane resistance $\rho_{zz}$ for examples of all of the superconducting samples studied. In each case, several field sweeps at fixed temperatures spanning the approximate range $0.5 \leqslant T \leqslant 4.2$ K are shown. (a) $M$=Cr, $Y$=$C_6H_5NO_2$, (b) $M$=Ga, $Y$=$C_6H_5NO_2$, (c) $M$=Fe, $Y$=$C_6H_5CN$.

former material. Indeed, for two out of the three $M$=Ga, $Y$=$C_6H_5NO_2$ crystals studied at high fields (those with higher Dingle temperatures—see Table I), the low-frequency oscillation was so indistinct as to make an accurate determination of the frequency impossible. On the other hand, when $M$=Cr and $Y$=$C_6H_5NO_2$, it is unambiguously clear that only a single series of oscillations is present [Fig. 3(a)].

In order to extract Fermi-surface cross-sectional areas from the Shubnikov–de Haas oscillations,[3] we define the oscillatory fraction of the magnetoresistance

$$\frac{\Delta R_{zz}}{R_{\mathrm{BG}}} = \frac{R_{zz} - R_{\mathrm{BG}}}{R_{\mathrm{BG}}}. \tag{2}$$

Here $R_{\mathrm{BG}}$ is the slowly varying background magnetoresistance, approximated by a polynomial in $B$. As long as $\Delta R_{zz}/R_{\mathrm{BG}} \ll 1$, $\Delta R_{zz}/R_{\mathrm{BG}} \approx -\Delta\sigma_{zz}/\sigma_{\mathrm{BG}}$, where the $\sigma$ are equivalent terms in the conductivity;[34] ($\Delta\sigma_{zz}/\sigma_{\mathrm{BG}}$ is the quantity dealt with in the Lifshitz-Kosevich (LK) treatment of Shubnikov–de Haas oscillations;[35,36] below we shall use the LK formalism to extract effective masses of the quasiparticles). The $\Delta R_{zz}/R_{\mathrm{BG}}$ values were processed using numerical Fourier transformation typically using data in the field range 7–32 T.

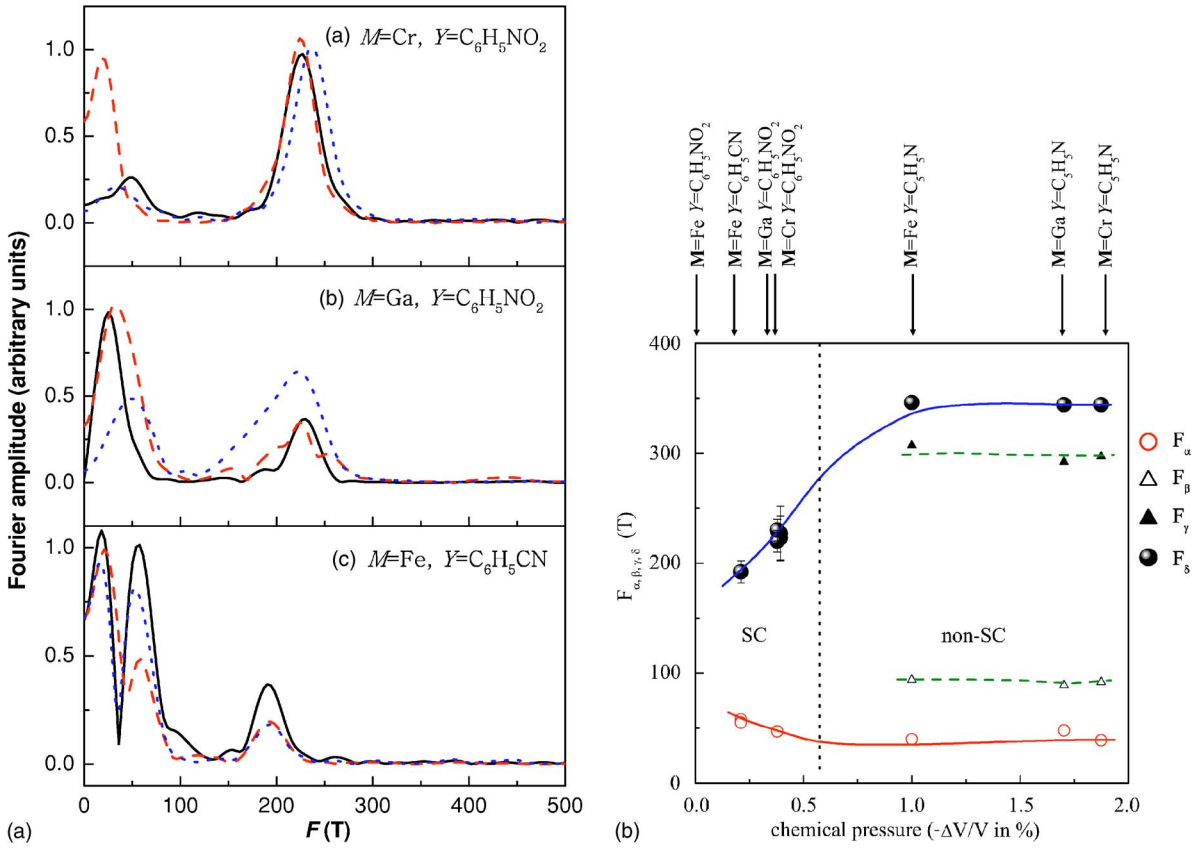


FIG. 4. (Color online) (Left panel) Fourier transforms of the oscillatory component of the resistivity at $\theta=0$ for (a) $M=\mathrm{Cr}$, $Y=\mathrm{C_6H_5NO_2}$, (b) $M=\mathrm{Ga}$, $Y=\mathrm{C_6H_5NO_2}$, and (c) $M=\mathrm{Fe}$, $Y=\mathrm{C_6H_5CN}$. The different curves are for different samples at $T\approx 0.5$ K. (Right panel) Summary of the SdH frequencies for the salts studied here and in Ref. 14; the labeling follows Ref. 14. The dotted line, which serves as a guide to the eye, separates the samples which are superconducting (SC: this study) from those which are non-superconducting (non-SC: Ref. 14; note that four distinct frequencies are observed in the salts of Ref. 14.

Some typical Fourier transforms are shown in Fig. 4, note that any apparent frequencies $F \lesssim 25$ T are almost certainly due to imperfections in the background subtraction procedure. Their amplitude and position depended critically on, for example, the order of polynomial used. For each material, the most prominent series of oscillations visible in Fig. 3 results in a well-defined peak in the Fourier spectrum with $F$ in the range 180–230 T (Fig. 4). Following the precedent set in Ref. 14 we label this frequency $F_\delta$. In addition, the $M=\mathrm{Ga}$, $Y=\mathrm{C_6H_5CN}$ [Fig. 4(b)] crystals and one of the $M=\mathrm{Fe}$, $Y=\mathrm{C_6H_5NO_2}$ samples [Fig. 4(c)] exhibit a second peak at $F\approx 50$ T, corresponding to the lower frequency of oscillations visible in Figs. 3(b) and 3(c). As noted above, this series of oscillations was less distinct in the other two $M=\mathrm{Ga}$, $Y=\mathrm{C_6H_5NO_2}$ crystals studied at high fields, leaving the corresponding peak in the Fourier transform difficult to identify with any confidence [Fig. 3(b)]. Again we follow the labelling convention in Ref. 14 and refer to this frequency as $F_\alpha$. Values of the frequencies are tabulated in Table I.

The magnetic-field-orientation dependence of the Shubnikov–de Haas oscillations (see Sec. III E—all frequencies vary as $1/\cos\theta$, where $\theta$ is the angle between the magnetic field and $c^*$), lead us to attribute the peaks in the Fourier transforms to quasi-two-dimensional Fermi-surface pockets. The Fermi surfaces of the salts in this study therefore only comprise one or two pockets, with the larger corresponding to a cross-sectional area ~5% of the Brillouin-zone cross-sectional area. By contrast, the isostructural $\beta''$-(BEDT-TTF)$_4$[$(\mathrm{H_3O})M(\mathrm{C_2O_4})_3$]$\cdot\mathrm{C_5H_5N}$ salts studied in Ref. 14 possess Fermi surfaces with four pockets, the areas of which obey the additive relationship expected for a compensated semimetal. The Shubnikov–de Haas oscillation frequencies observed in the salts measured in this paper and those of the $\beta''$-(BEDT-TTF)$_4$[$(\mathrm{H_3O})M(\mathrm{C_2O_4})_3$]$\cdot\mathrm{C_5H_5N}$ salts are summarized in the lower panel of Fig. 4. Following the convention of Ref. 14, we label the larger-area Fermi surface pocket of the $\beta''$-(BEDT-TTF)$_4$[$(\mathrm{H_3O})M(\mathrm{C_2O_4})_3$]$\cdot Y$ salts $\delta$, and the smaller one (if present) $\alpha$.

Band-structure calculations on this family of salts predict two Fermi-surface pockets, of equal area (roughly 8.5% of the Brillouin zone);[14,37] by contrast, the experimental data shown in Figs. 4(a)–4(c) suggest one or two rather smaller pockets, with unequal area. There are a number of possible reasons for this difference. First, while extended-Hückel calculations often give a reasonable qualitative description of the Fermi surfaces of many BEDT-TTF salts,[3] the $\beta''$ phases have proved problematic; slight differences in input parameters seem to result in wildly differing predicted topologies [see, e.g., the case of $\beta''$-(BEDT-TTF)$_2$AuBr$_2$ (Ref. 38)]. Second, the band-structure calculations employ lattice pa-

rameters measured at relatively high temperatures;[17] lattice contraction could result in changes in the relative sizes of the various transfer integrals, leading to shifts in the bands with respect to the chemical potential. Third, the smaller than expected pockets could be a consequence of a Fermi-surface reconstruction associated with one of the features observed in the temperature dependence of the resistivity (e.g., that at $T_{MI}$—see Fig. 1). Analogous Fermi-surface reconstructions have been suggested for other $\beta''$ salts, including $\beta''$-(BEDT-TTF)$_2$AuBr$_2$ (where a plethora of small Fermi surface pockets results),[38] the $\beta''$-(BEDT-TTF)$_4$[(H$_3$O)$M$(C$_2$O$_4$)$_3$]·C$_5$H$_5$N salts,[14] and $\beta''$-(BEDT-TTF)$_2$SF$_5$CH$_2$CF$_2$SO$_3$; in the latter case it appears that the Fermi-surface nesting is more efficient.[39]

As in the case of the $\beta''$-(BEDT-TTF)$_4$[(H$_3$O)$M$(C$_2$O$_4$)$_3$]·C$_5$H$_5$N salts,[14] the appearance of the Shubnikov–de Haas oscillations is affected by $M$, with the lower-frequency series being much more visible for $M$=Fe [see Figs. 3(b) and 3(c)]. This may be related to relatively small differences in the scattering mechanisms, rather than some intrinsic effect of the $Fe^{3+}$ ion. Examples of similar effects have been observed elsewhere; e.g., Ref. 40 discusses magnetoresistance data for the low-field, low-temperature phases of $\alpha$-(BEDT-TTF)$_2$KHg(SCN)$_4$ and $\alpha$-(BEDT-TTF)$_2$TlHg(SCN)$_4$, taken from the works of several different groups; the relative amplitudes of the various Shubnikov–de Haas oscillation series vary from sample to sample, and batch to batch, with some series being undetectable in what is presumed to be the the lower-quality samples, whilst being relatively strong in other crystals.

### D. Other Fermi-surface parameters

A two-dimensional Lifshitz-Kosevich formula[36] has been used to extract the effective masses $m^*$ of the various Fermi-surface pockets, where possible.[41] The Fourier amplitude of each series of quantum oscillations is given by

$$A_{2D} \propto R_T R_D R_S, \tag{3}$$

where $R_T = X/\sinh(X)$ is the temperature damping term, $R_D = \exp[-X(T_D/T)]$ is the Dingle term ($T_D$ is the Dingle temperature) due to the broadening of the Landau levels caused by internal inhomogeneities and $X = 14.694(T/B)(m^*/m_e)$. The spin splitting term $R_S = |\cos\{(\pi/2)[g^* m^*/m_e/\cos(\theta)]\}|$, where $g^*$ is the effective $g$ factor, will be dealt with below.

Figure 5 shows the temperature dependence of the Fourier amplitude of the oscillations attributed to the larger Fermi-surface pocket as a function of temperature for the three different salts. We find consistently that the effective mass is clearly enhanced in the systems containing magnetic ions from $m^* = 1.23 \pm 0.02 m_e$ to $m^* = 1.7 \pm 0.1 m_e$, when $M$=Ga and $M$=Cr, respectively, with $Y$=C$_6$H$_5$NO$_2$, and to $m^* = 1.6 \pm 0.1 m_e$ for $M$=Fe and $Y$=C$_6$H$_5$CN (see Fig. 5 and Table I). This is possibly similar to the case of $\kappa$-(BETS)$_2$FeCl$_4$, where it was proposed that spin fluctuation effects enhanced the effective mass,[42] but in contrast to the isostructural $\beta''$-(BEDT-TTF)$_4$[(H$_3$O)$M$(C$_2$O$_4$)$_3$]·C$_5$H$_5$N salts,[14] in which there is no detectable enhancement when $M$=Cr or Fe. This suggests that the effective masses of the superconducting salts are perhaps more sensitive to renormalization, due to the presence of the magnetic ions, than those of the nonsuperconducting $\beta''$-(BEDT-TTF)$_4$[(H$_3$O)$M$(C$_2$O$_4$)$_3$]·C$_5$H$_5$N salts.

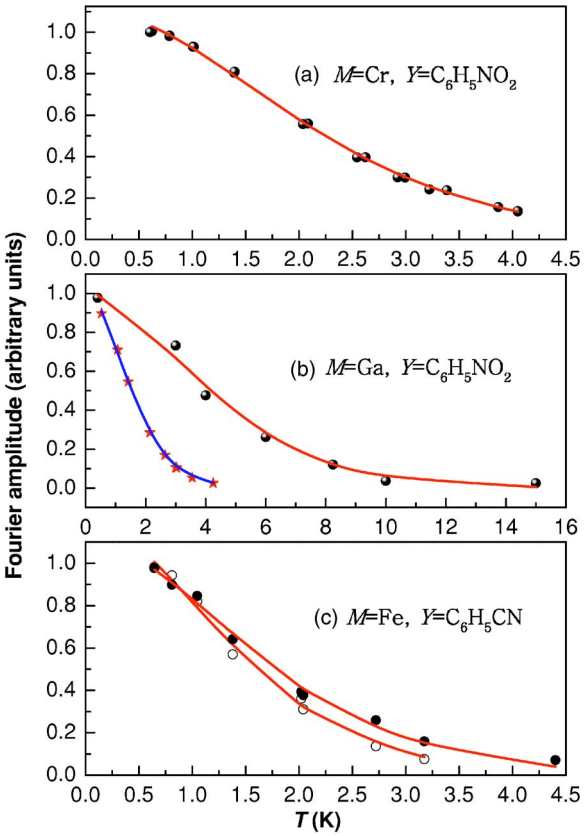


FIG. 5. (Color online) Temperature dependence of the Fourier amplitude of the higher-frequency $F_\delta$ Shubnikov–de Haas oscillation series. In each case, data are shown as points and the curves are fits to the $R_T$ part of Eq. (3). (a) $M$=Cr, $Y$=C$_6$H$_5$NO$_2$; the field window is 20–33 T, fitted by $m^* = 1.6 \pm 0.1 m_e$. (b) $M$=Ga, $Y$=C$_6$H$_5$NO$_2$; the solid points correspond to Fourier transforms covering a field window of 25–56 T, fitted by $m^* = 1.24 \pm 0.05 m_e$ and the star points cover a field window 10–16.7 T, fitted by $m^* = 1.22 \pm 0.05 m_e$. (c) $M$=Fe, $Y$=C$_6$H$_5$CN; the two data sets are for the $\alpha$ and $\delta$ pockets using the same field window (10–33 T); the fits give $m^* = 1.4 \pm 0.1 m_e$ (closed circles) and $m^* = 1.6 \pm 0.1 m_e$ (open circles), respectively.

The Dingle temperatures $T_D$ obtained for the superconducting salts studied in the present work do not show a systematic dependence on the identity of the $M$ ion (see Table I); variations from sample to sample of the same material are just as great as variations from salt to salt. A similar observation was made for the isostructural, nonsuperconducting $\beta''$-(BEDT-TTF)$_4$[(H$_3$O)$M$(C$_2$O$_4$)$_3$]·C$_5$H$_5$N salts;[14] however, the Dingle temperatures of the samples in this work are consistently higher than those of the $\beta''$-(BEDT-TTF)$_4$[(H$_3$O)$M$(C$_2$O$_4$)$_3$]·C$_5$H$_5$N salts studied in Ref. 14. This difference may be due to the higher quasiparticle density of the latter salts, which could result in better screening of disorder.

Another similarity between $\beta''$-(BEDT-TTF)$_4$[(H$_3$O)$M$(C$_2$O$_4$)$_3$]·C$_5$H$_5$N salts and the salts in this

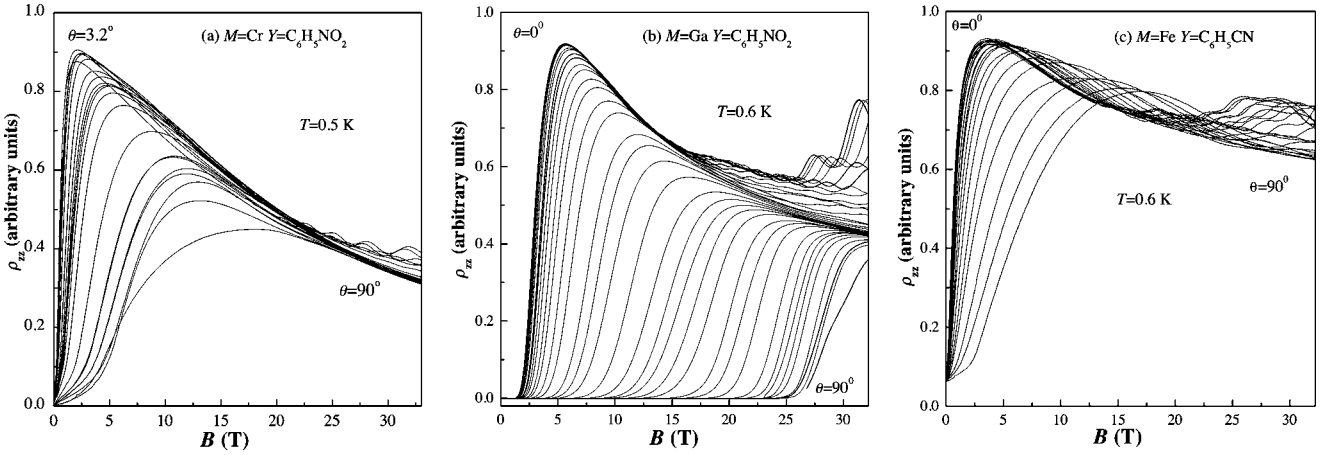


FIG. 6. The field dependence of the interlayer resistance $\rho_{zz}$ as a function of angle $\theta$ between $c^*$ (the normal to the conducting $ab$ planes) and the applied magnetic field at $T \approx 0.5$ K for (a) $M$=Cr, $Y$=$C_6H_5NO_2$, (b) $M$=Ga, $Y$=$C_6H_5NO_2$, and (c) $M$=Fe, $Y$=$C_6H_5CN$. Several fixed $\theta$ sweeps are shown, with the upper and lower $\theta$ limits displayed in the figure.

work is the lack of correlation between the Dingle temperature and the ratio $\rho_{zz}(T)/\rho_{zz}(293\ \mathrm{K})$; given the mixed-phase nature of these systems, the Dingle temperature will give a gauge of only the quality of the *metallic* regions of the samples, whereas the $\rho_{zz}(\mathrm{T})/\rho_{zz}(286\ \mathrm{K})$ values will depend on the relative proportion of insulating *and* metallic domains within the crystals.

### E. Angle-dependent magnetoresistance and effective $g$ factor

Figure 6 shows the interplane resistivity $\rho_{zz}$ versus magnetic field at several fixed angles $\theta$ between $c^*$, the normal to the conducting planes ($ab$), and the magnetic field. As expected for a quasi-two-dimensional system, the frequency of the quantum oscillations increases as $F \propto 1/\cos\theta$ [see the inset to Fig. 7(a)]. Note also that the superconducting upper critical field, taken, as above, to be the resistivity maximum, moves upwards as $\theta$ increases.

The $\theta$ dependence of the Fourier amplitude of the $\delta$ series of Shubnikov–de Haas oscillations is plotted for each salt in Fig. 7. The $R_S$ term in Eq. (3) leads to minima in the amplitude of the oscillations at angles $\theta$ given by[35]

$$(2n+1) = \frac{1}{\cos(\theta)} g^* m^*, \tag{4}$$

where $n$ is an integer. This is often known as a spin zero. Spin zeros can be seen clearly in Figs. 7(b) and 7(c); fitting these to Eq. (3) yields $g^*m^* = 2.1 \pm 0.1$ for $M$=Ga, $Y$=$C_6H_5NO_2$ and $g^*m^* = 1.8 \pm 0.2$ for $M$=Fe, $Y$=$C_6H_5CN$ (see Table I). Unfortunately the $\alpha$ series of Shubnikov–de Haas oscillations were insufficiently well defined for a reliable estimate of $g^*m^*$ to be made.

Figure 8 shows the $\theta$ dependence of the interlayer resistivity $\rho_{zz}$ at fixed field. For each sample, the data comprise a slowly varying background, upon which is superimposed Shubnikov–de Haas oscillations (generally largest close to $\theta$=0°) and features due to the superconductivity (the sharp dips $\theta$=90°). These features showed little dependence on the plane of rotation of the sample in the magnetic field. In contrast to charge-transfer salts in which the Fermi surface is unambiguously three dimensional [e.g., $\kappa$-(BEDT-TTF)$_2$Cu(NCS)$_2$ (Ref. 9)], the $\beta''$-(BEDT-TTF)$_4$[$(H_3O)M(C_2O_4)_3$]$\cdot Y$ salts do not exhibit angle-

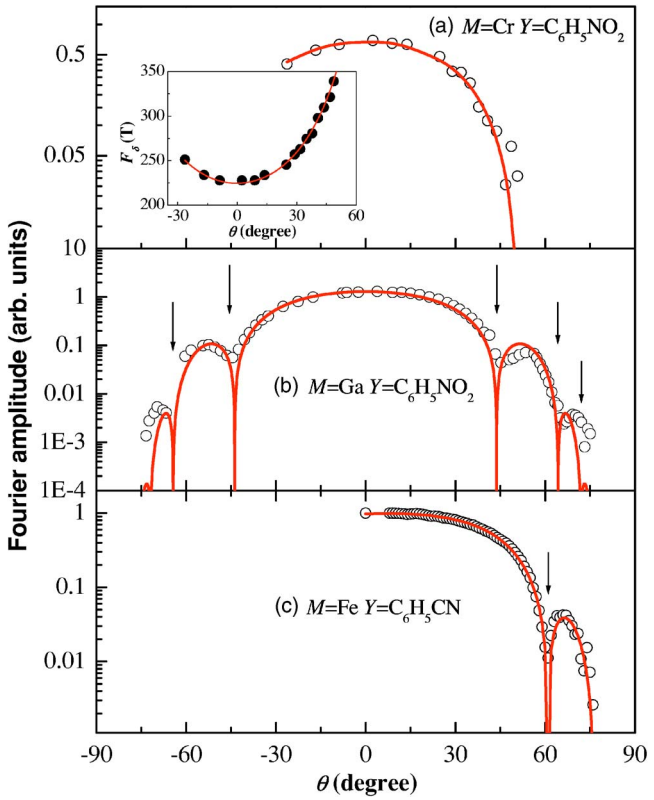


FIG. 7. (Color online) Angle dependence of the Fourier amplitude of the $\delta$ frequency at $T$=0.5 K; the amplitudes correspond to transforms of data spanning 12 to 42 T. The figures are for (a) $M$=Cr, $Y$=$C_6H_5NO_2$, (b) $M$=Ga, $Y$=$C_6H_5NO_2$, and (c) $M$=Fe, $Y$=$C_6H_5CN$; the solid lines are fits to Eq. (3) and the arrows indicate the position of the spin zeros. The inset to (a) shows a typical $\theta$ dependence of the Shubnikov–de Haas oscillation frequency (in this case for $M$=Cr, $Y$=$C_6H_5NO_2$); solid line is a fit to $F=F_0/\cos(\theta)$ with $F_0$=224 T.

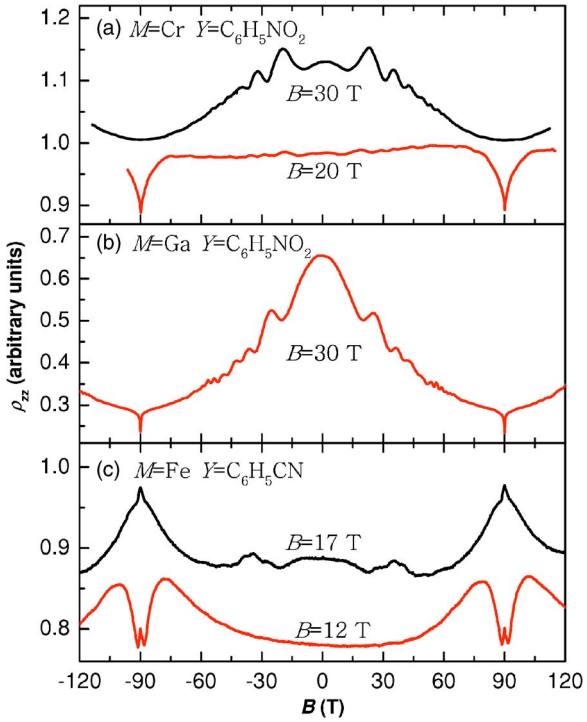


FIG. 8. (Color online) Angle dependence of $\rho_{zz}$ at fixed field and temperature ($T$=0.5 K) for (a) $M$=Cr, $Y$=$C_6H_5NO_2$ (sample C), (b) $M$=Ga, $Y$=$C_6H_5NO_2$ (sample B), and (c) $M$=Fe, $Y$=$C_6H_5CN$ (sample A). The fixed field used is labeled in the figure.

dependent magnetoresistance oscillations (AMROs) due to the field-induced motion of quasiparticles across Fermi sheets possessing corrugations with an interlayer component.[9] The apparent lack of AMRO is probably due to the large anion layer in these materials that reduces the degree of molecular orbital overlap between layers, giving rise to incoherent transport in the interlayer direction. The AMRO data show no evidence of "hidden" sections of Fermi surface that are not apparent in the field-dependent data.

### F. Anisotropy of the superconducting upper critical field

As has been mentioned above, the exact location of the transition from the superconducting to normal states of the $\beta''$-(BEDT-TTF)$_4$[$(H_3O)M(C_2O_4)_3$]$\cdot Y$ superconductors is difficult to define because of the peak in $R_{zz}(\propto\rho_{zz})$ and its associated negative magnetoresistance, plus the generally broadened nature of the transition (see, e.g., Fig. 10). To obtain a qualitative understanding of the magnetic-field-orientation dependence of the upper critical field, we therefore follow previous precedents[3,32] and use the positions of the peak in $R_{zz}$ and the midpoint of the resistive transition as two measures of the *resistive* upper critical field.

Following these definitions, Fig. 9 shows the temperature dependences of the interplane critical field $B_{c2\perp}$ ($\theta$=0, i.e., $B\|I\|c^*$) and in-plane critical field $B_{c2\|}$ ($\theta$=90°, i.e., $B\perp I\|c^*$), for $\beta''$-(BEDT-TTF)$_4$[$(H_3O)Ga(C_2O_4)_3$]$\cdot C_6H_5NO_2$. Both $B_{c2\perp}$ and $B_{c2\|}$ decrease with increasing temperature $T$, $B_{c2\|}$ varying roughly linearly; the intercept at $T\rightarrow 0$ is $B_{c2\|}$=33.1±0.4 T (peak field) and $B_{c2\|}$=29.8±0.5 T (midpoint field). The corresponding slopes are $dB_{c2\|}/dT\approx -3.8$ T/K and $\approx -5$ T/K for the peak and midpoint fields, respectively. Similar linear $B_{c2\|}(T)$ dependences have been observed in *resistive* measurements of the $\kappa$-(BEDT-TTF)$_2X$ superconductors (e.g., Refs. 15 and 43).

By contrast, the resistive $B_{c2\perp}(T)$ exhibits a concave temperature dependence, describable by $B_{c2\perp}\propto(T_c-T)^n$ with $n>1$ (see Fig. 9). Such behavior is observed in the resistive transition of a number of organic superconductors (see Sec. IV of Ref. 3 and references therein for a summary); it suggests that the temperature dependence of the resistive transition is more closely related to the irreversibility line than to the true upper critical field. The difference between the resistive transition defined by the peak and the true $B_{c2}$ derived from thermodynamic or penetration-depth measurements is least significant at low temperatures (Ref. 3, and references therein), and so the discussion of the anisotropy of the upper critical field of the $\beta''$-(BEDT-TTF)$_4$[$(H_3O)M(C_2O_4)_3$]$\cdot Y$ salts below employs data recorded at $T\approx 0.5$ K.

The anisotropy of the resistive upper critical field was investigated by sweeping the magnetic field at fixed angles $\theta$ and at a temperature 0.5 K (see Fig. 10). Figure 10 shows the resulting angle dependence of the resistive $B_{c2}$; both midpoint and peak-position data are shown in (b). In common with other BEDT-TTF superconductors,[3,43] the $\theta$ dependence of the resistive upper critical field may be adequately fitted by either an anisotropic three-dimensional Ginzburg-Landau expression[44]

$$1=\left(\frac{B_c(\theta)\cos(\theta)}{B_{c2\perp}}\right)^2+\left(\frac{B_c(\theta)\sin(\theta)}{B_{c2\|}}\right)^2 \quad (5)$$

or by Tinkham's expression for superconducting thin films[44]

$$1=\left|\frac{B_c(\theta)\cos(\theta)}{B_{c2\perp}}\right|+\left(\frac{B_c(\theta)\sin(\theta)}{B_{c2\|}}\right)^2, \quad (6)$$

with the latter giving a slightly superior-quality fit close to $\theta$=90° when the parameters $B_{c2\perp}$=5.24±0.05 T and $B_{c2\|}$=33.37±0.15 T (peak) and $B_{c2\perp}$=3.13±0.04 T and $B_{c2\|}$=29.65±0.14 T (midpoint) are used [Fig. 10 (inset)].

Although Eqs. (5) or (6) can give a reasonable fit to the $\theta$-dependent resistive $B_{c2}$ data, their apparent success cannot be taken as a justification for the applicability of the physics underlying either Equation to the $\beta''$-(BEDT-TTF)$_4$[$(H_3O)M(C_2O_4)_3$]$\cdot Y$ salts. Whereas the upper critical field of quasi-two-dimensional BEDT-TTF superconductors is limited by orbital effects for most orientations of the field, the in-plane upper critical field is usually limited by spin effects.[3,15,26,43] Consequently, a literal interpretation of the fit parameters of Eq. (5) will give an apparent orbital anisotropy that is orders of magnitude too small.[39,43] Moreover, the dissipative mechanisms giving rise to the peak in $R_{zz}$ are unlikely to be the same for in-plane and out-of-plane fields,[39] as evidenced by the distinct temperature dependences of the resistive critical fields (Fig. 9) and the rather different appearance of the peak at 90% (see Fig. 6) compared to other $\theta$ values.

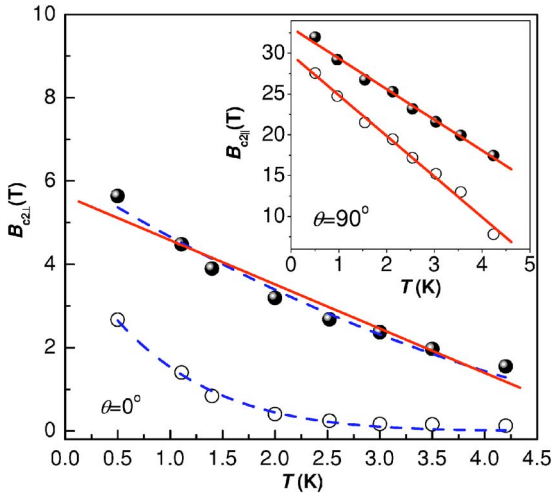


FIG. 9. (Color online) Temperature dependence of the in-plane ($B_{c2\perp}$) and interplane ($B_{c2\parallel}$—see inset) resistive upper critical fields of $\beta''$-(BEDT-TTF)$_4$[$(H_3O)Ga(C_2O_4)_3$]·$C_6H_5NO_2$. Values derived from the position of the peak in $R_{zz}$ are shown as solid circles; values corresponding to the midpoint of the resistive transition are plotted as open circles. The dashed lines are fits to the power laws of the form $B_{c2} \propto (T-T_c)^n$, as described in the text; the solid lines are linear fits.

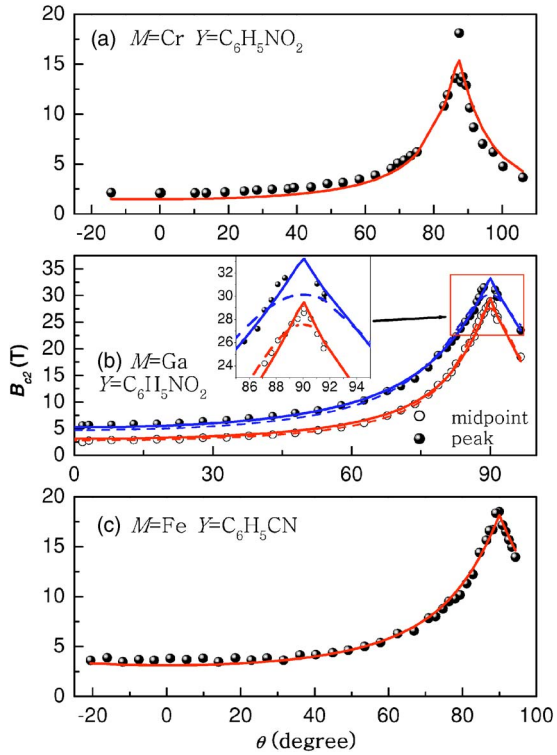


FIG. 10. (Color online) Angle dependence of the resistive upper critical field $B_{c2}$ extracted from the peak position (solid circles) and midpoint position between the superconducting and normal regions (open circles) at $T$=0.5 K. Solid lines are fits to Eq. (6) and dashed lines are fits to Eq. (5). (a) $M$=Cr, $Y$=$C_6H_5NO_2$, (b) $M$=Ga, $Y$=$C_6H_5NO_2$, (c) $M$=Fe, $Y$=$C_6H_5CN$.

Figure 10 compares resistive $B_{c2}(\theta)$ data for the $M$=Ga, $Y$=$C_6H_5NO_2$, $M$=Cr, $Y$=$C_6H_5NO_2$, and $M$=Fe, $Y$=$C_6H_5CN$ salts. Interestingly, the presence of a magnetic ion on the $M$ site appears to greatly affect the in-plane resistive critical field. Whereas the $M$=Ga, $Y$=$C_6H_5NO_2$ salt has $B_{c2\parallel} \approx 33$ T, comfortably exceeding the Pauli paramagnetic limit ($\approx$19 T for $T_c \approx 7$ K),[32,43] the equivalent critical fields for the salts with $M$=Cr and $M$=Fe are almost a factor 2 lower (see also Table I).

## IV. DISCUSSION

Reference 14 pointed out the role of intrinsic disorder in both the $\beta''$-(BEDT-TTF)$_4$[$(H_3O)M(C_2O_4)_3$]·$Y$ salts and the $\kappa$-(BEDT-TTF)$_2X$ superconductors; at temperatures just above superconductivity, both families of salts exhibit states that have been classed as "unconventional" or "bad" metals. As mentioned above, such states may represent a mixture of "insulating" and "metallic" behavior or coexisting phases. However, rather than dealing with their similarities, in the current paper we shall instead concentrate on the *differences* between the superconductivity in the $\beta''$-(BEDT-TTF)$_4$[$(H_3O)M(C_2O_4)_3$]·$Y$ and $\kappa$-(BEDT-TTF)$_2$ salts.

First of all, in the $\kappa$-(BEDT-TTF)$_2X$ salts, there is a strong connection between superconducting parameters such as $T_c$ and $B_{c2}$ and the quasiparticle effective mass. For example, increases in pressure decrease the effective mass and also reduce $T_c$;[7,8,45] irrespective of the exact details of the mechanism for superconductivity, it is believed[3] that the decrease in the quasiparticle density of states at the Fermi energy (indicated by the reduction in effective mass) is responsible, at least in part, for the suppression of the superconductivity. By contrast, inspection of Table I shows that there is little correlation between $m^*$ and $T_c$ or $B_{c2}$. Indeed, the superconducting salt with the lightest mass ($M$=Ga, $Y$=$C_5H_5NO_2$) exhibits the largest value of the in-plane critical field by almost a factor 2.

Second, the superconductivity occurs in the $\beta''$-(BEDT-TTF)$_4$[$(H_3O)M(C_2O_4)_3$]·$Y$ salts at a very low carrier density and density of states compared to other BEDT-TTF superconductors, but the in-plane upper critical fields of $\kappa$-(BEDT-TTF)$_2$Cu(NCS)$_2$ and $\beta''$-(BEDT-TTF)$_4$[$(H_3O)Ga(C_2O_4)_3$]·$C_6H_5NO_2$ are virtually the same.[32] This is despite the fact that the areal carrier density and the quasiparticle density of states of the former are significantly larger than those of the latter (comparing the quantum-oscillation frequencies[45] and effective masses, respectively). One could also compare critical temperatures; in spite of the very large differences in quasiparticle density and densities of states, the $T_c$'s of the two materials are within 30% of one another. Apparently, something other than a large density of quasiparticle states at the Fermi energy is important in sustaining superconductivity in the $\beta''$-(BEDT-TTF)$_4$[$(H_3O)M(C_2O_4)_3$]·$Y$ salts.

Finally, disorder seems to play only a small part in determining the superconducting properties. In spite of relatively large differences in sample quality [as suggested by $\rho_{zz}(T \rightarrow 0)/\rho_{zz}(293\ \mathrm{K})$ ; see Fig. 1] and the Dingle temperature (see Table I), there seems to be little difference in $T_c$ or $B_{c2}$ between samples of the same composition. This is in contrast

to the situation in $\kappa$- and $\beta$-phase (BEDT-TTF) superconductors,[2] where nonmagnetic impurities and disorder are thought to suppress the superconductivity.

It appears, therefore, that there are distinct differences between the mechanism for superconductivity in the $\beta''$-(BEDT-TTF)$_4$[$(H_3O)M(C_2O_4)_3$]$\cdot Y$ salts that are the subject of the present paper and the $\kappa$-(BEDT-TTF)$_2X$ salts.

A clue as to the mechanism responsible is given by examining Fig. 1 in conjunction with Table II, which shows the unit-cell volumes of the materials studied in this work and in Ref. 14. First, the material with the largest unit cell, $M$ =Fe, $Y$=$C_6H_5NO_2$, shows little or no tendency towards metallic behavior; for all temperatures $\leqslant$120 K, $d\rho_{zz}/dT$ is negative (inset in Fig. 1). Moving to slightly smaller unit cell sizes, the relative change in $\rho_{zz}$ between room temperature and the peak close to $T_c$ varies significantly from $\sim$1 or 2 for $M$=Ga, $Y$=$C_6H_5NO_2$ and $M$=Cr, $Y$=$C_6H_5NO_2$ [Figs. 1(a) and 1(b)] to $\sim$8 for $M$=Cr, Fe, $Y$=$C_6H_5CN$ [Fig. 1(c)]. This suggests that the fraction of the metallic component decreases and the activated, insulating regions become more dominant as the unit cell size increases. In other words, the $\beta''$-(BEDT-TTF)$_4$[$(H_3O)M(C_2O_4)_3$]$\cdot Y$ salts tend to more insulating behavior, the larger the unit cell.[46] Further support for this idea is found in the latter part of Sec. III A, where activation energies $E_A$ were used to describe the insulating component of the resistivity (see Table I) of the superconducting salts. Note that, the fitted $E_A$ is largest for $M$ =Fe, $Y$=$C_6H_5CN$; a qualitatively similar variation in $T_{MI}$ is also observed, with $T_{MI}\approx 70-80$ K for $M$=Ga, Cr, $Y$ =$C_6H_5NO_2$ and $T_{MI}\approx$120 K for $M$=Fe, $Y$=$C_6H_5CN$. As suggested above, the more metallic tendencies (lower $T_{MI}$ and $E_A$) are exhibited by the salts with smaller unit cells [$M$=Ga or Cr, $Y$=$C_6H_5NO_2$ salt unit-cell volumes 7145.2 and 7144.4 Å$^3$, respectively], while the salt with the largest unit cell (7169.6 Å$^3$) is the completely "insulating" $M$ =Fe, $Y$=$C_6H_5NO_2$ compound. Lastly, we note that further increases in unit-cell size result in a larger quasiparticle density (four Fermi-surface pockets), and the cessation of superconductivity (see Fig. 4, right panel).[14]

A final indication as to the origin of the superconductivity is given by the Raman scattering data shown in Fig. 11 for the salt with $M$=Ga and $Y$=$C_6H_5NO_2$. As the temperature is lowered, the $\nu_2$ mode peak at 1492 cm$^{-1}$ splits at $\sim$100 K, with the splitting becoming more pronounced as the temperature is decreased further. The splitting of the $\nu_2$ mode peak is indicative of charge ordering and is observed in a number of the $\beta''$-(BEDT-TTF)$_4$[$(H_3O)M(C_2O_4)_3$]$\cdot Y$ family of salts, though the splitting of the peak is not as pronounced in the nonsuperconducting salts This signature of charge ordering occurs at around the same temperature where the transport shows a crossover from metallic to insulating behavior at $T_{MI}$ (see Fig. 1 and Ref. 14. The results of the Raman investigation gives further weight to the idea that the phase diagram of these salts is similar to the one proposed by Ref. 1, where the superconducting phase is bounded by a charge ordered phase on one side and a metallic phase on the other, tuned by the ratio $V/t$. A more detailed discussion of the Raman scattering results and the results of infrared reflectance spectroscopy performed on the $\beta''$-(BEDT-TTF)$_4$[$(H_3O)M(C_2O_4)_3$]$\cdot Y$ family of salts will be published elsewhere.[47]

TABLE II. Unit cell volumes $V$ of selected $\beta''$-(BEDT-TTF)$_4$[$(H_3O)M(C_2O_4)_3$]$\cdot Y$ salts ($C2/c$ symmetry group) measured around 120 K (after Ref. 14.

| $M/Y$ | $V$(Å$^3$) |
|---|---|
| Fe/$C_6H_5NO_2$ | 7169.6 |
| Fe/$C_6H_5CN$ | 7157 |
| Ga/$C_6H_5NO_2$ | 7145.2 |
| Cr/$C_6H_5NO_2$ | 7144.4 |
| Cr/$C_6H_5CN$ | 7121.6 |
| Fe/$C_5H_5N$ | 7101.0 |
| Ga/$C_5H_5N$ | 7051.9 |

To summarize, the $\beta''$-(BEDT-TTF)$_4$[$(H_3O)M(C_2O_4)_3$]$\cdot Y$ salt with the largest unit-cell size is an insulator; subsequent slight decreases in unit-cell size allow the salts to take on a partially metallic character, and exhibit superconductivity. Further decreases suppress the superconductivity and raise the quasiparticle number density. Therefore, rather than a large quasiparticle density of states (as seems necessary for superconductivity in the $\kappa$-phase BEDT-TTF superconductors[3]), it appears that proximity to an insulating state characterized by charge order is the most important prerequisite for superconductivity in the $\beta''$-(BEDT-TTF)$_4$[$(H_3O)M(C_2O_4)_3$]$\cdot Y$ salts. Very similar behavior is observed in the charge-density-wave system (BEDT-TTF)$_3$Cl$_2$.2H$_2$O (Ref. 21) as the pressure is increased; in that case, it was tentatively suggested that the superconductivity was mediated by charge fluctuations.[34]

The evolution of the superconductivity in the both classes of salts with unit-cell size is entirely characteristic of the predictions of the model of Ref. 1. In this scenario, a charge-ordered state is adjacent to a metallic phase; the parameter that tunes from one phase to the other is $V/t$, the ratio of the nearest-neighbor Coulomb repulsion energy $V$ to the average transfer integral $t$. As the unit cell size decreases, $t$ will tend to grow faster than $V$, leading to a transition from charge order (high $V/t$) to metallic behavior. The phase boundary

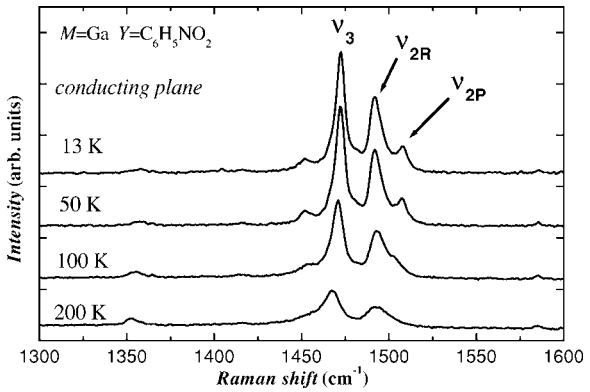


FIG. 11. Raman spectra of $\beta''$-(BEDT-TTF)$_4$[$(H_3O)$Ga$(C_2O_4)_3$]$\cdot C_6H_5NO_2$ taken at fixed temperatures in the range $13\leqslant T\leqslant 200$ K.

between these regions ends at a quantum-critical point as $T \rightarrow 0$; in the region around this point, superconductivity mediated by charge fluctuations occurs. We suggest that the systematic variation of physical properties of the $\beta''$-(BEDT-TTF)$_4$[$(H_3O)M(C_2O_4)_3$]$\cdot Y$ salts with unit-cell volume indicates that this mechanism is the cause of the superconductivity.

## V. CONCLUSION

We have described a series of magnetoresistance experiments on charge-transfer salts of the form $\beta''$-(BEDT-TTF)$_4$[$(H_3O)M(C_2O_4)_3$]$\cdot Y$, concentrating on those with $Y = C_6H_5CN$ and $C_6H_5NO_2$. The (magneto)transport data show that the salts with $M$=Ga, Cr, $Y = C_6H_5NO_2$ and $M$=Fe, $Y = C_6H_5CN$ are superconductors, and that the properties of these compounds can be understood by proposing that they are electronically inhomogeneous, consisting of coexisting metallic and insulating phases. In spite of this "intrinsic disorder," prominent Shubnikov–de Haas oscillations are observed at low temperatures and high magnetic fields, showing that the superconducting salts possess Fermi surfaces with one or two small quasi-two-dimensional pockets, their total area comprising $\lesssim 6\%$ of the room-temperature Brillouin zone. The quasiparticle effective masses were found to be enhanced when the ion $M$ was magnetic (Fe or Cr). In spite of the very low quasiparticle density [$\lesssim 10\%$ of that in the $\kappa$-(BEDT-TTF)$_2X$ superconductors] and the relatively small effective masses, the superconductivity in the $\beta''$-(BEDT-TTF)$_4$[$(H_3O)M(C_2O_4)_3$]$\cdot Y$ salts is rather robust, with $T_c \approx 7$ K and in-plane upper critical fields of between 18 and 33 T, the latter being comparable to the highest critical fields of *any* BEDT-TTF superconductor. The systematic variation of the properties of the $\beta''$-(BEDT-TTF)$_4$[$(H_3O)M(C_2O_4)_3$]$\cdot Y$ salts with unit-cell volume points to the possibility that the mechanism for superconductivity in these salts is the charge-fluctuation-mediated one proposed by Merino and McKenzie.[1]

## ACKNOWLEDGMENTS

This work was supported by EPSRC (UK), the Royal Society (UK), JSPS (Japan), and by the U.S. Department of Energy (DOE) under Grants Nos. LDRD 20030084DR and LDRD 2004099ER. Work at the National High Magnetic Field Laboratory was performed under the auspices of the National Science Foundation, the State of Florida, and DOE. We thank Steve Blundell, Jason Lashley, Ross McKenzie, and Albert Migliori for fruitful discussions.

*Present address: Research Centre for Spectrochemistry, Graduate School of Science, The University of Tokyo, Hongo, Bunkyo-ku, Tokyo, 113-0033, Japan.

†Present address: Department of Material Science, Graduate School and Faculty of Science, Himeji Institute of Technology, Hyogo 678-1297, Japan.

[1] Jaime Merino and R. H. McKenzie, Phys. Rev. Lett. **87**, 237002 (2001).

[2] B. J. Powell and R. H. McKenzie, Phys. Rev. B **69**, 024519 (2004).

[3] J. Singleton and C. H. Mielke, Contemp. Phys. **43**, 63 (2002).

[4] S. Lefebvre, P. Wzietek, S. Brown, C. Bourbonnais, D. Jerome, C. Meziere, M. Fourmigue, and P. Batail, Phys. Rev. Lett. **85**, 5420 (2000).

[5] F. Kagawa, T. Itou, K. Miyagawa, and K. Kanoda, Phys. Rev. B **69**, 064511 (2004).

[6] G. Kotliar, E. Lange, and M. J. Rozenberg, Phys. Rev. Lett. **84**, 5180 (2000).

[7] H. Weiss, M. V. Kartsovnik, W. Biberacher, E. Steep, E. Balthes, A. G. M. Jansen, K. Andres, and N. D. Kushch, Phys. Rev. B **59**, 12370 (1999).

[8] R. D. McDonald, A.-K. Klehe, J. Singleton, and W. Hayes, J. Phys.: Condens. Matter **15**, 5315 (2003).

[9] P. A. Goddard, S. J. Blundell, J. Singleton, R. D. McDonald, A. Ardavan, A. Narduzzo, J. A. Schlueter, A. M. Kini, and T. Sasaki, Phys. Rev. B **69**, 174509 (2004).

[10] A. F. Bangura, P. A. Goddard, S. Tozer, A. I. Coldea, R. D. McDonald, J. Singleton, A. Ardavan, and J. Schlueter, Synth. Met. (to be published).

[11] B. J. Powell and R. McKenzie, J. Phys.: Condens. Matter **16**, L367 (2004).

[12] G. Varelogiannis, Phys. Rev. Lett. **88**, 117005 (2002).

[13] A. Girlando, M. Masino, A. Brillante, R. G. DellaValle, and E. Venuti, Phys. Rev. B **66**, 100507(R) (2002).

[14] A. I. Coldea, A. F. Bangura, J. Singleton, A. Ardavan, A. Akutsu-Sato, H. Akutsu, S. S. Turner, and P. Day, Phys. Rev. B **69**, 085112 (2004).

[15] J. Singleton, J. A. Symington, M.-S. Nam, A. Ardavan, M. Kurmoo, and P. Day, J. Phys.: Condens. Matter **12**, L641 (2000).

[16] M. Kurmoo, A. W. Graham, P. Day, S. J. Coles, M. B. Hursthouse, J. Caulfield, J. Singleton, F. L. Pratt, W. Hayes, L. Ducasse, and P. J. Guionneau, J. Am. Chem. Soc. **117**, 12 209 (1995).

[17] H. Akutsu, A. Akutsu-Sato, S. S. Turner, D. Le Pevelen, P. Day, V. Laukhin, A.-K. Klehe, J. Singleton, D. A. Tocher, M. R. Probert, and J. A. K. Howard, J. Am. Chem. Soc. **124**, 12 430 (2002).

[18] S. S. Turner, P. Day, K. M. A. Malik, M. B. Hursthouse, S. J. Teat, E. J. Maclean, L. Martin and S. A. French, Inorg. Chem. **38**, 3543 (1999).

[19] T. Yamamoto, M. Uruichi, K. Yakushi, J. I. Yamaura, and H. Tajima, Phys. Rev. B **70**, 125102 (2004).

[20] Several crystals of each compound were measured as there were significant variations in properties even between samples from the same batch. This is a common feature of charge-transfer salts in which there are interstitial solvent molecules; such materials tend to have a greater degree of macroscopic inhomogeneity due to the loss of solvent over time. Our large data set, comprising measurements of many crystals over an extended period of time gives us confidence that the data presented represent typical

properties for each composition, irrespective of sample age or batch.

[21] W. Lubczynski, S. V. Demishev, J. Singleton, J. M. Caulfield, L. du Croo de Jongh, C. J. Kepert, S. J. Blundell, W. Hayes, M. Kurmoo, and P. Day, J. Phys.: Condens. Matter **8**, 6005 (1996).

[22] S. J. C. Yates, G. Santi, S. M. Hayden, P. J. Meeson, and S. B. Dugdale, Phys. Rev. Lett. **90**, 057003 (2003); C. Pfleiderer *et al.*, Nature (London) **412**, 58 (2001).

[23] J. Dumas and C. Schlenker, Int. J. Mod. Phys. B **7**, 4045 (1993).

[24] T. Sasaki, N. Toyota, M. Tokumoto, N. Kinoshita, and H. Anzai, Solid State Commun. **75**, 93 (1990).

[25] J. Singleton, C. H. Mielke, W. Hayes, and J. A. Schlueter, J. Phys.: Condens. Matter **15**, L203 (2003).

[26] S. Rashid, S. S. Turner, P. Day, J. A. K. Howard, P. Guionneau, E. J. L. McInnes, F. E. Mabbs, R. J. H. Clark, S. Firth and T. Biggs, J. Mater. Chem. **11**, 2095 (2001).

[27] P. Goddard, S. W. Tozer, J. Singleton, A. Ardavan, A. Abate, and M. Kurmoo, J. Phys.: Condens. Matter **14**, 7345 (2002).

[28] M.-S. Nam, S. J. Blundell, A. Ardavan, J. A. Symington, and J. Singleton, J. Phys.: Condens. Matter **13** 2271 (2001).

[29] N. E. Hussey, H. Takagi, Y. Iye, S. Tajima, A. I. Rykov, and K. Yoshida, Phys. Rev. B **61**, R6475 (2000).

[30] F. Zuo, J. A. Schlueter, and J. M. Williams, Phys. Rev. B **60**, 574 (1999).

[31] X. Su, F. Zuo, J. A. Schlueter, J. M. Williams, P. G. Nixon, R. W. Winter, and G. L. Gard, Phys. Rev. B **59**, 4376 (1999).

[32] M.-S. Nam, J. A. Symington, J. Singleton, S. J. Blundell, A. Ardavan, J. A. A. J. Perenboom, M. Kurmoo, and P. Day, J. Phys.: Condens. Matter **11** L477 (1999).

[33] S. Friemel, C. Pasquier, and D. Jerome, Physica C **292**, 273 (1997).

[34] J. Singleton, Rep. Prog. Phys. **63**, 1111 (2000).

[35] D. Shoenberg, *Magnetic Oscillations in Metals* (Cambridge University Press, Cambridge, UK, 1984).

[36] N. Harrison, R. Bogaerts, P. H. P. Reinders, J. Singleton, S. J. Blundell, and F. Herlach, Phys. Rev. B **54**, 9977 (1996); N. Harrison, A. House, I. Deckers, J. Caulfield, J. Singleton, F. Herlach, W. Hayes, M. Kurmoo, and P. Day, *ibid.* **52**, 5584 (1995).

[37] T. G. Prokhorova, S. S. Khasanov, L. V. Zorina, L. I. Buravov, V. A. Tkacheva, A. A. Basakakov, R. B. Morgunov, M. Gerer, E. Canadell, R. P. Shibaeva, and E. B. Yagubskii, Adv. Funct. Mater. **13**, 403 (2003).

[38] A. A. House, N. Harrison, S. J. Blundell, I. Deckers, J. Singleton, F. Herlach, W. Hayes, J. A. A. J. Perenboom, M. Kurmoo, and P. Day, Phys. Rev. B **53**, 9127 (1996).

[39] M.-S. Nam, A. Ardavan, J. A. Symington, J. Singleton, N. Harrison, C. H. Mielke, J. A. Schlueter, R. W. Winter, and G. L. Gard, Phys. Rev. Lett. **87**, 117001 (2001).

[40] N. Harrison, E. Rzepniewski, J. Singleton, P. J. Gee, M. M. Honold, P. Day, and M. Kurmoo, J. Phys.: Condens. Matter **11**, 7227 (1999).

[41] To verify the validity of the analysis of the quantum oscillations, in the absence of de Haas–van Alphen data, Lifshitz-Kosevich analysis was also performed on the raw Shubnikov–de Haas oscillation amplitudes, i.e., without division by the nonoscillatory background. The results of this procedure were found to agree with the conventional analysis reported in the text to within the experimental errors.

[42] N. Harrison, C. H. Mielke, D. G. Rickel, L. K. Montgomery, C. Gerst, and J. D. Thompson, Phys. Rev. B **57**, 8751 (1998).

[43] F. Zuo, J. S. Brooks, R. H. McKenzie, J. A. Schlueter, and J. M. Williams, Phys. Rev. B **61**, 750 (2000).

[44] M. Tinkham, *Introduction to Superconductivity* (Krieger, Malabar, Fl, 1975).

[45] J. M. Caulfield, W. Lubczynski, F. L. Pratt, J. Singleton, D. Y. K. Ko, W. Hayes, M. Kurmoo, and P. Day, J. Phys.: Condens. Matter **6**, 2911 (1994).

[46] Evidence of this dependence on the unit cell volume has also been observed in pressure dependent data obtained on the $\beta''$-(BEDT-TTF)$_4$[$(H_3O)Ga(C_2O_4)_3$]$\cdot C_6H_5NO_2$ salt. This salt becomes more metallic upon application of pressure and exhibits magnetoresistance similar to the smaller unit cell volume $\beta''$-(BEDT-TTF)$_4$[$(H_3O)M(C_2O_4)_3$]$\cdot C_5H_5N$ salts, that were the subject of Ref. 14. We would like to thank Dr. A-K. Klehe and Dr. V. Laukin for allowing us to see this data in advance of publication.

[47] T. Yamamoto *et al.* (unpublished).